Synthesis of Manganese Oxide Electrodes with Interconnected Nanowire Structure as an Anode Material for Rechargeable Lithium Ion Batteries

Mao-Sung Wu,*,† Pin-Chi Julia Chiang,‡ Jyh-Tsung Lee,‡ and Jung-Cheng Lin‡

Department of Chemical and Material Engineering, National Kaohsiung University of Applied Sciences, Kaohsiung 807-78, Taiwan, Republic of China, and Materials Research Laboratories, Industrial Technology Research Institute, Hsinchu 310, Taiwan, Republic of China

Received: August 22, 2005; In Final Form: October 13, 2005

Manganese oxide electrodes composed of interconnected nanowires are electrochemically synthesized in manganous acetate solution at room temperature without any template and catalyst. Annealing temperature affects the electrode morphology, crystallization, and electrochemical performance. Scanning electron microscope (SEM) results show that nanowires are uniformly distributed and sizes are about 12−18 nm in diameter; the diameter decreases to about 8−12 nm after annealing at 300 °C. X-ray diffraction (XRD) and transmission electron microscope (TEM) images indicate that nanowires have poor crystalline characteristics. The higher the annealing temperature, the higher the crystalline degree is in manganese oxide. The synthesized anode material shows a much larger capacity than the traditional graphite materials for lithium storage. After annealing at 300 °C, the electrode's reversible capacity reaches 800 $mAhg^{-1}$, and the specific capacity retention remains nearly constant after 100 cycles.

Introduction

Graphite materials are currently used as some of the anode materials for rechargeable lithium ion batteries, in which lithium ions intercalate in and out reversibly. Graphite materials provide high capacity, high electronic conductivity, and low electrochemical potential with respect to lithium metal. Yet these superb properties still can hardly meet the demand of high-energy density from electronic devices nowadays; researches on alternative anodes are therefore focused on materials of higher lithium storage capacities. Among the candidates, metal oxides have attracted much attention due to their advantageously high capacities.

Idota et al.[1] reported a new type of high-capacity anode material that consists of tin-based amorphous oxides. Tin-based oxides, thereafter, have been intensively investigated.[2−5] Recently, Poizot et al.[6,7] proposed a class of new anode materials, the nanosized transition-metal oxides, for lithium ion batteries. The electrodes made of nanoparticles of transition-metal oxides (MO, where M is Co, Ni, Cu, or Fe) demonstrate high electrochemical capacities (about 700 $mAhg^{-1}$), great capacity retention, and high recharging rates. More importantly, the mechanism of Li reactivity differs from the classical Li insertion/deinsertion or Li-alloying processes. The mechanism involves the formation and decomposition of Li_2O, accompanying the reduction and oxidation of metal nanoparticles, respectively.[6] Wang et al.[8] reported that nanosized cobalt oxides (Co_3O_4) synthesized by chemical decomposition of cobalt octacarbonyl in toluene at low temperature are nanosized and demonstrate a stable reversible lithium storage capacity of 360 $mAhg^{-1}$ within 30 cycles. Another example of a nanocrystalline NiO thin-film electrode prepared by pulsed laser ablation shows a reversible capacity of 700 $mAhg^{-1}$ in the range of 0.01−3.0 V vs Li/Li^+. A high capacity retention up to 100 cycles may be achieved by optimizing the NiO films.[9] Improved specific capacity, discharge rate, and cycling performance have been attributed to the nanosized character of the thin-film electrode of NiO.

On the basis of the above, nanosized anode materials (transition-metal oxides) play an important role in facilitating the reduction and oxidation between Li_2O and the metal nanoparticle during charging/discharging. Therefore, synthesis of nanosized anode materials has become very important. In this work, we synthesized the interconnected manganese oxide nanowire electrode electrochemically as a new anode material, in which the production cost is low and fabrication is easy. Hitherto, manganese oxide material has rarely been reported as an anode material for rechargeable lithium ion batteries. Yet the natural abundance of manganese oxide and its environmental compatibility are so advantageous that it should not be neglected as a promising electrode material in various energy storage devices.

In practice, an electrode composed of nanoparticle is more difficult to fabricate due to the poor dispersibility of nanoparticles in slurry (composed of organic solvent, nanoparticles, polymer binder, and conducting agent, etc.). Here, nanosized manganese oxide electrodes consisting of interconnected nanowires are electrochemically synthesized onto nickel substrates at room temperature without any template and catalyst. The proposed electrochemical deposition technique has a great advantage over the others because mass and thickness of the metal oxide film can be easily controlled by adjusting the current, bath chemistry, and temperature. Material structure and electrochemical performance of the electrode are also investigated.

Experimental Section

Previous results showed that morphology of the electrodeposited manganeseoxide is affected by the applied potential

* To whom correspondence should be addressed. E-mail: ms_wu@url.com.tw. Fax: 886-7-3830674.
† National Kaohsiung University of Applied Sciences.
‡ Industrial Technology Research Institute.

10.1021/jp054740b CCC: $30.25
Published on Web 11/10/2005

between the working and the reference electrodes, in which current density varies during deposition.[10,11] In this study, a constant current density was applied to deposit the active material; therefore by measuring the deposition time, one could control the weight of manganese oxide precisely. The resultant electrode morphology and structure were different from any of the previous results. A saturated calomel electrode (SCE) was used as the reference electrode and a platinum foil with dimension 2 × 2 cm^2 was used as the counter electrode. Nanostructured manganese oxide electrodes were deposited onto nickel foils (1 × 1 cm^2) by applying a current density of 0.25 mA cm^{-2} in a solution bath of 0.1 M manganous acetate and 0.1 M sodium sulfate for 10 min at room temperature.[10−13] The plating solution was stirred continuously by a Teflon stir on a hot plate during the deposition. After deposition, plated foils were rinsed several times in deionized water and dried at 100, 300, and 500 °C for 1 h in air. The amount of deposited manganese oxide was measured by a microbalance. The amount of manganese oxide as an anode material in a Li cell was about 0.12 mg cm^{-2} measured by electronic microbalance (Mettler, AE101-S). The anode was double-sided, therefore the total amount of manganese oxide was about 0.24 mg. All experiments were carried out in a three-compartment cell.

Surface morphology of the deposited electrode was examined with a scanning electron microscope (SEM, LEO-1530) with an accelerating voltage of 4 keV. Crystal structures of the deposited manganese oxide were identified by X-ray powder diffraction (XRD, Philips PW1700) with a Cu Kα target (wavelength = 1.54056 Å). Diffraction data were collected for 1 s at each 0.04° step width over 2θ, ranging from 20° to 80°. Nanostructure of the manganese oxide was further examined with a transmission electron microscope (FE-TEM, JEOL JEM-2100F) with an accelerating voltage of 200 kV. The TEM specimen was prepared via the following procedure: nanowires were stripped off and dispersed in anhydrous ethanol with ultrasonic vibration for 5 min, a drop of the supernatant was then transferred onto a standard holey carbon-covered-copper TEM grid. An X-ray photoelectron spectroscopy (Perkin-Elmer, PHI Quantera SXM) with a focused monochromatic Al Kα radiation (1486.6 eV) was used to analyze the composition of the deposited manganese oxide electrode. Thermogravimetric (TGA) measurement was carried out in air at a heating rate of 10 °C min^{-1} on a thermal analyzer (Perkin-Elmer, TGA7).

Batteries were assembled in a dry room. The electrochemical cell was comprised of a working electrode (manganese oxide electrode), a counter electrode (lithium metal), and a reference electrode (lithium metal). A working electrode wrapped with separator (Celgard 2320, 20 μm in thickness) was placed between two counter electrodes and then inserted into an aluminum−plastic laminated film case. Electrolyte was injected into the case that was then sealed off at a reduced pressure. The electrolyte was 1 M lithium hexafluorophosphate ($LiPF_6$, Tomiyama Pure Chemical) in ethylene carbonate/propylene carbonate/diethylene carbonate (EC/PC/DEC = 1/1/2, by volume). The water content of the electrolyte was less than 10 ppm, measured via the Karl Fischer titration technique in an argon-filled glovebox.

Electrochemical tests were performed on a charge/discharge unit (Maccor model series 4000). Cells were charged at a constant current (85 mA g^{-1}) to a cutoff potential of 10 mV vs Li/Li^+. Discharge was performed at the same rate to a cutoff potential of 2.0 V vs Li/Li^+. Cyclic voltammetry (CV) measurements were taken by means of a potentiostat/galvanostat (Schlumberger SI 1286). The potential was cycled in the range of 0.01 to 2.0 V vs Li/Li^+, with a scan rate of 0.1 mV s^{-1}.

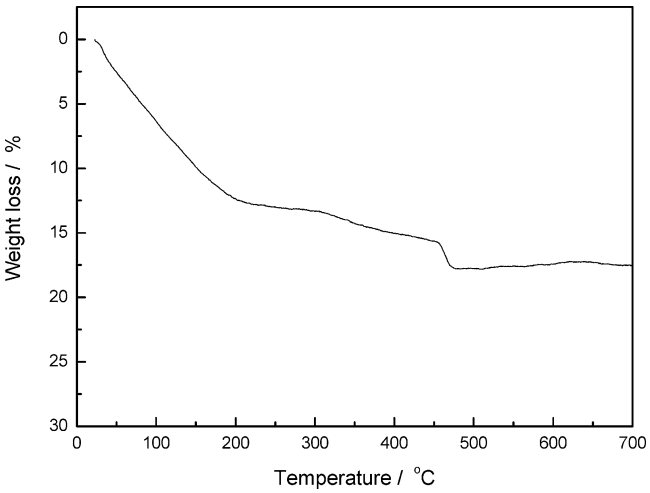

Figure 1. Typical TGA behavior of a synthesized manganese oxide electrode in air.

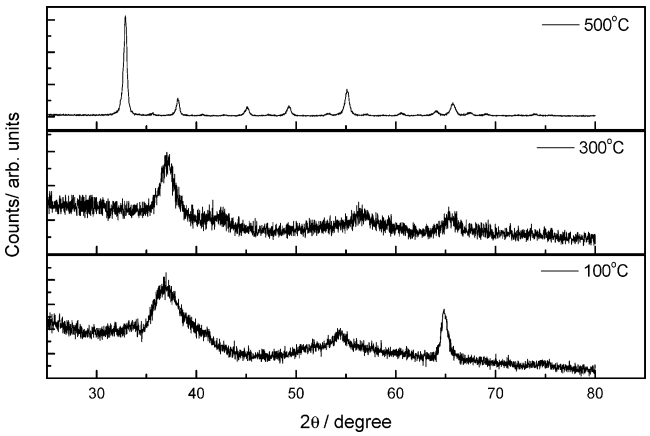

Figure 2. XRD patterns of a synthesized manganese oxide electrode after different annealing temperatures.

Results and Discussion

Figure 1 shows typical TGA behavior of the synthesized manganese oxide electrode in air. An 18% weight loss at a temperature higher than 500 °C has been detected. The apparent weight loss from room temperature to 200 °C corresponds to the loss of hydrated water (about 11%).[14] According to Preisler,[15] only a small percentage of water in electrodeposited manganese dioxide is volatile at 120 °C, and a predominant portion of water is desorbed in a relatively smooth manner up to 350 °C. The electrodeposited manganese oxide decomposes rapidly to form Mn_2O_3 at temperatures beyond 500 °C.[14] Water content within is known to affect the electrochemical reactivity and the thermodynamic stability of various manganese oxide phases as it causes variations in crystal lattice and consequently in electrical conductivity and electrode potential.[13,16] Moreover, water in the electrode material structure creates challenges in lithium battery application because of the instability of lithium with water and the decomposition of water during the charge/discharge processes.

Figure 2 shows the XRD patterns of the deposited manganese oxide after different annealing temperatures. The XRD patterns of 100 and 300 °C resemble closely those of γ-$Mn(O,OH)_2$ (γ-manganese oxide hydroxide, JCPDS 17-0510), while the pattern for 500 °C resembles more that of Mn_2O_3 (manganese oxide,

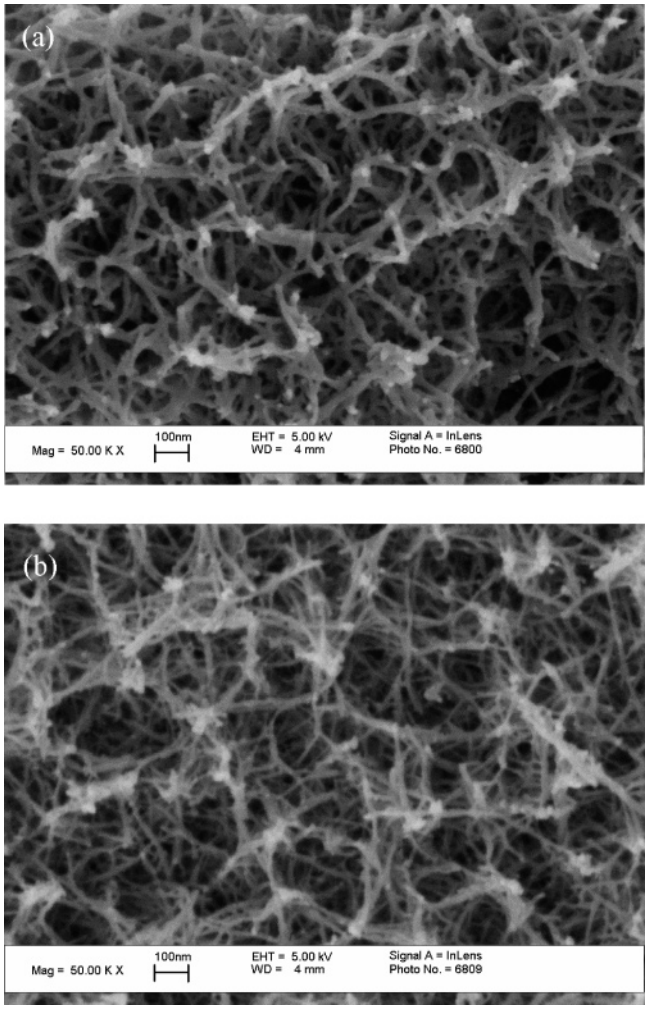

Figure 3. SEM micrograph of a manganese oxide electrode after different annealing temperatures: (a) 100 and (b) 300 °C.

JCPDS 24-0508). This structural difference confirms that the deposited manganese oxide decomposes to Mn_2O_3 at temperatures beyond 500 °C, corresponding to the TGA results. To avoid structural destruction from water contamination, the annealing temperature has been set at 300 °C or below. The XRD peak at about $2\theta = 37.1$ ° becomes broader as the annealing temperature decreases from 300 to 100 °C; such a widening indicates a poor crystallinity and a decrease of the average grain size by the decrease in annealing temperature. The mean grain size of the deposited manganese oxide was calculated by using Scherrer's equation with the diffraction peak at $2\theta = 37.1°$: $D = 0.9\lambda/(\beta \cos \theta)$, where λ is the X-ray wavelength, β is the full width at half-maximum (fwhm), and θ is the Bragg angle. The calculated grain size at 100 and 300 °C is 1.6 and 2.4 nm, respectively.

Figure 3 shows an SEM micrograph of the manganese oxide electrode after different annealing temperatures. Electrodes are highly porous and composed of interconnected nanowires. Nanowires are uniformly distributed and are about 12−18 nm in diameter after annealing at 100 °C (Figure 1a); the diameter decreases to about 8−12 nm after annealing at 300 °C (Figure 1b). The morphology of the deposited manganese oxide electrode is clearly affected by the annealing temperature. Increasing the annealing temperature decreases the diameter of nanowires. The change in morphology after higher temperature annealing may be attributed to the removal of both the surface and the structural water from the solid phase of the manganese oxide structure.

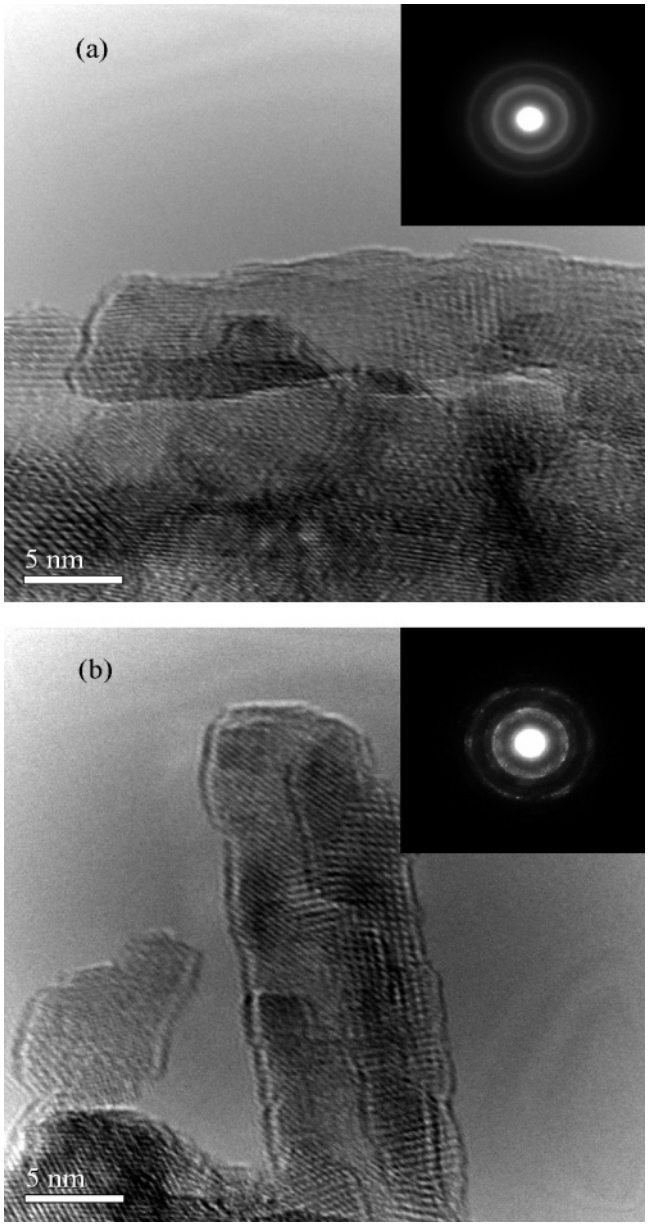

Figure 4. TEM and SAD (selected area diffraction) observations of manganese oxide nanowire after (a) 100 and (b) 300 °C treatments.

According to Preisler,[15,17] γ-manganese dioxides, which exhibit a marked growth orientation and a fibrous structure as well as cleavability, are deposited on the anodes during electrolysis of manganous salt solutions in a sulfate bath. Therefore, the γ-manganese dioxides are fibrous or wire-structured in nature. Our previous results showed that γ-manganese oxides could form different types of nanowire structure at anodic deposition by the cyclic voltammetric method in a sulfate bath containing manganous salt solutions.[18] At a low potential range of 0.1 to 0.4 V vs SCE (lower current density), the synthesized manganese oxides were vertical nanowires. At a potential range higher than 0.5 V vs SCE (higher current density), the synthesized manganese oxides tended to form an interconnected nanowire.[18] In this work, we synthesized the manganese oxide electrodes using the constant current anodic deposition method at a high current density of 0.25 mA cm^{-2} with a corresponding potential over 0.5 V vs SCE; consequently, the interconnected nanowire structure is obtained.

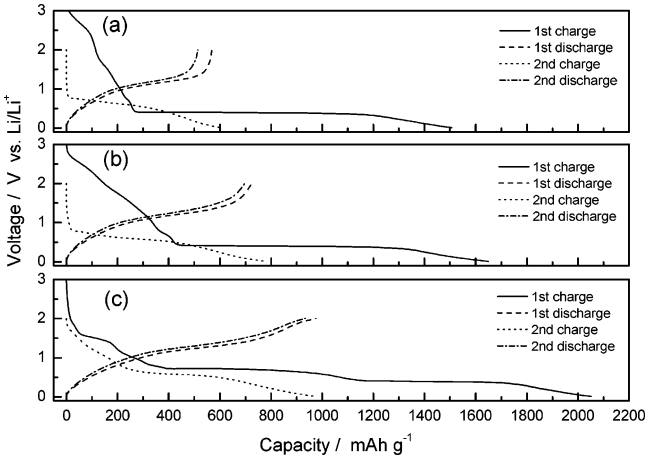

Figure 5. The voltage−capacity curves of the manganese oxide electrodes. Electrodes are treated at (a) 100, (b) 300, and (c) 500 °C before the test.

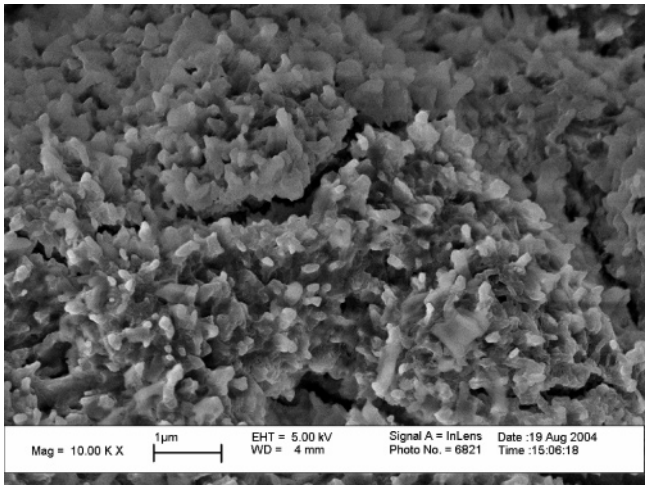

Figure 6. EM morphology of a 300 °C treatment of the manganese oxide electrode after its first charging cycle.

Figure 4 shows the TEM andSAD (selected area diffraction) observations of the manganese oxide nanowires after annealing at 100 and 300 °C. Both TEM patterns (lattice images) show that the manganese oxide nanowires are crystalline structured. Ring diffraction patterns from polycrystalline manganese oxides show that the rings are made up of discrete spots (Figure 4b) after 300 °C treatment, meaning that the deposited manganese has higher crystallinity than that of the 100 °C treatment. A less crystalline structure produces a more continuous ring pattern (Figure 4a), indicating that annealing not only removes water content but also causes the changes in the degree of crystallinity of material.

The purpose of this work is not only to synthesize a nanostructured manganese oxide electrode but to propose a plausible anode material for lithium ion batteries, which means that a study of the electrode's electrochemical performance must be done. Figure 5 shows the voltage−capacity curves of the manganese oxide electrodes after annealing at different temperatures. Capacity is measured between 0.01 and 2.0 V vs Li/Li^+. During the first charge process, potentials in both electrodes drop rapidly to plateau (about 0.4V), then decrease continuously to 0.01V. In the first discharge process, both voltage readings increase with no significant plateau, and lower capacity values are achieved compared to their corresponding charge capacity values. The reversible capacity after annealing at 100 °C is about 600 mAh g^{-1} (Figure 5a). After annealing at 300 °C (Figure 5b), the reversible capacity reaches about 800 $mAhg^{-1}$, which is twice that of a typical graphite anode (about 372 $mAhg^{-1}$). The manganese oxides at 500 °C annealing are structurally different from the manganese oxides annealed below 300 °C (Figure 2). Data show that the 500 °C annealing electrodes not only remain chargeable, but also contain a higher capacity (Figure 5c). The reversible capacity after annealing at 500 °C is about 970 mAh g^{-1} (Figure 5c). The one drawback yet to be overcome is the large irreversible capacity. After the first charge/discharge cycle, both electrodes demonstrate a small irreversible capacity in each sequential cycle. According to the charge/discharge behaviors of transition metal oxide,[6] the second charge curve differs considerably from the first because there have been some drastic, lithium-driven, and structural or textural modifications. The large irreversible capacity occurring only in the first cycle may be caused by decomposition reactions of the electrolyte and formation of the SEI (solid electrolyte interphase) film onto the surface of the manganese oxide electrode.[19] Figure 6 shows the SEM morphology of the manganese oxide electrode treated at 300 °C after the first charging cycle. Clearly the electrode morphology has been changed drastically. This morphological change shows that the lithium-storage process in the manganese oxide electrode is unlike the process in lithiated compounds such as graphite materials, because the morphology of graphite after lithium intercalation does not change significantly, with only a small volumetric expansion. Since the rock-salt-structured crystal of 3d transition metal oxides has no empty sites for lithium ions to intercalate into, nor can it form alloys with lithium, these metal oxides show a completely new mechanism different from the classical ones.[6]

The reaction mechanism of manganese oxide with lithium has been proposed as follows, with reference to the transition metal oxide,[6]

$$MnO_2 + 4Li^+ + 4e^- \leftrightarrow 2Li_2O + Mn \quad (1)$$

$$4Li \leftrightarrow 4\,Li^+ + 4e^- \quad (2)$$

$$MnO_2 + 4Li \leftrightarrow 2Li_2O + Mn \quad (3)$$

Accordingly, the reaction between lithium and manganese oxide (a transition metal oxide) resulting in lithium oxide and manganese is thermodynamically feasible (eq 1).[6] In reality, however, Li_2O is electrochemically inactive, which means that to extract lithium from Li_2O is thermodynamically impossible. Yet the extraction may be plausible by using nanosized materials.[6] On the basis of this assumption, the electrochemically driven size confinement of the metal particles is thus believed to have enhanced effects on electrochemical activities in the formation/decomposition of Li_2O. Increasing the amount of metal atoms on the particle surface enhances the electrochemical reactivity of the particle by reducing its size. Therefore, the high capacity of the 300 and 500 °C annealing electrode is attributed to the small diameter (the nanowire of smaller diameter has a higher specific area for reaction in every unit weight) in manganese oxide nanowires as compared with that of the 100 °C annealing electrode (Figure 1).

To further understand the electrochemical mechanism of the reactions between manganese oxide electrode and lithium, XPS measurement has been applied to examine the valence change of manganese before and after lithium storage, or charge process, of the electrode as shown in Figure 7. Prior to measurements, the electrode has been charged to 0.01 V vs Li/Li^+. The two significant peaks of binding energies correspond to Mn $2p_{1/2}$

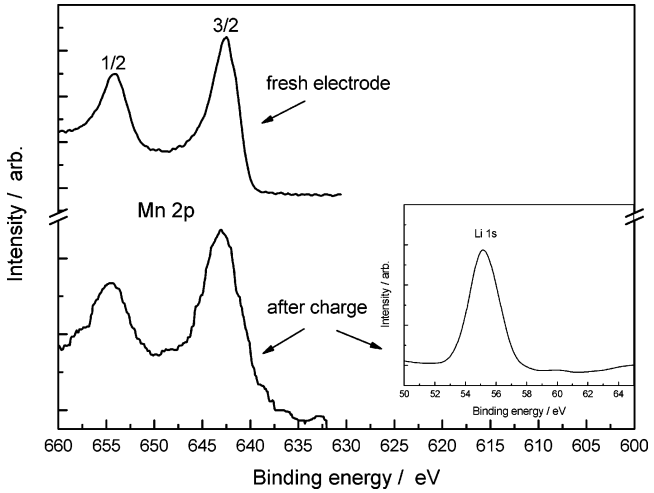

Figure 7. XPS spectra of a 300 °C treatment of the nanosized manganese oxide electrode before and after the first cycle charging.

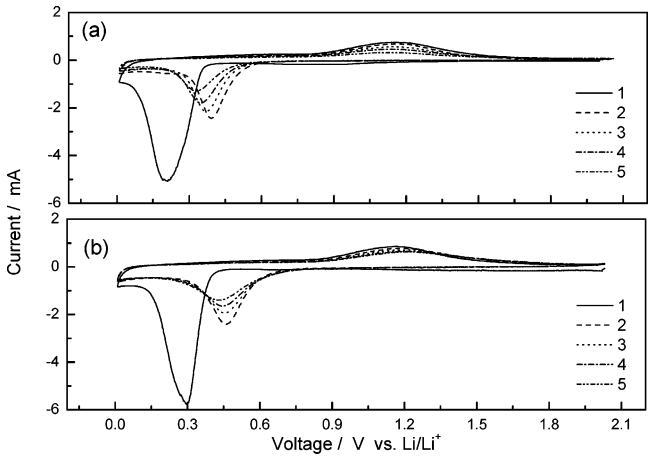

Figure 8. The 5-cycle CV curves of a manganese oxide electrode treated at different temperatures: (a) 100 and (b) 300 °C.

and Mn $2p_{3/2}$, respectively. The XPS spectrum shows broader peaks of Mn 2p binding energy than that of the fresh manganese oxide electrode, indicating a conversion of manganese oxide to metallic manganese. The Li 1s XPS spectrum for the electrode is also presented in the insert of Figure 7. The binding energy peak of 55.3 eV assigned to Li 1s, which attributes to Li_2O (55.6 eV), confirms the formation of Li_2O. The XPS result supports that manganese metal and Li_2O were formed during the initial charge process. Similar results in the study of the NiO and lithium reaction by XPS have been reported.[9]

Other electrochemical performance has been studied in addition to capacity determination. Figure 8 shows the CV curves of the manganese oxide electrode after annealing at different temperatures for five cycles. Clearly the first scan cycle, especially for the cathodic process, is different from all the other subsequent scanning cycles. The peak potential in the first cathodic scan locates at 0.2 V vs Li/ Li^+ and it shifts significantly to 0.4 V vs Li/ Li^+ after the first cycle. Peak current decreases too. This drastic cathodic peak potential change is related to the charge/discharge curves in Figure 5 and is attributed to structural or textural modifications due to the formation of Li_2O and metallic manganese. One can see a broad anodic peak in the second cycle at about 1.2 V vs Li/Li^+ on the anodic process, and a fairly sharp cathodic peak at 0.4 V vs Li/Li^+ on the cathodic process. These two peaks might be attributed by the reversible electrochemical oxidation and

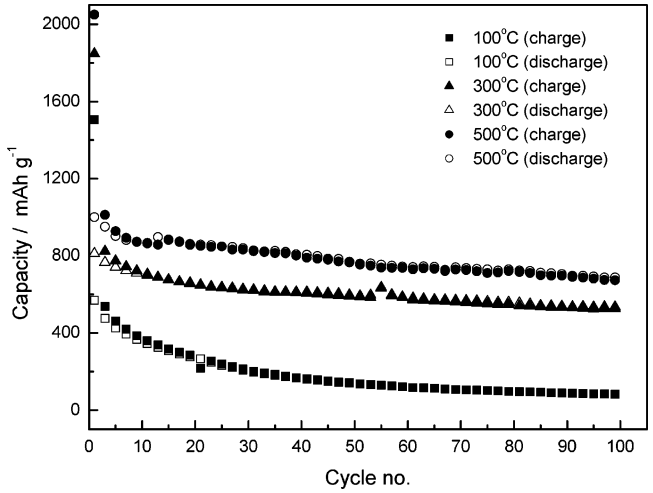

Figure 9. The relationship between specific capacity and cycle number of a manganese oxide electrode treated at different temperatures: 100, 300, and 500 °C.

reduction of manganese oxide with lithium in the electrode. For the 100 °C annealing electrode, the intensity of reduction and oxidation peaks gradually decreases in the subsequent scanning cycles. The 300 °C annealing electrode, on the other hand, remains stable throughout. One possibility is the reaction between the structural water in the electrode and lithium during the charging process, which forms a thick SEI film over the manganese particle surface to prevent reaction of manganese and Li_2O. Compared with other transition metal oxides in the literature, the manganese oxide electrode with interconnected nanowires has lower reduction and oxidation potentials vs Li/ Li^+ (0.4 and 1.2V) than those of NiO (0.9 and 2.3 V).[9,20] In general, lower reduction and oxidation potentials deliver higher energy density, an example being the graphite materials.

Figure 9 shows the capacity retention of the manganese oxide electrode after annealing at different temperatures. The specific capacity of manganese oxide after 300 and 500 °C annealing decreases in the first 10 cycles, then decays very slowly to a nearly constant capacity. The capacity of the electrode after 100 °C annealing, on the other hand, decreases rapidly in the first 40 cycles or so, then decays to a much lower capacity value. It is understandable and predictable that the hydrated water content affects the cycle-life performance. The capacity efficiencies in both electrodes are very high except for the first cycle, meaning that almost all the charged capacity can be discharged. A decrease in capacity indicates an increased electrode resistance with increasing cycle number. A possible reason is that during the charge/discharge processes, catalytic manganese metal may be isolated by the nonconducting materials such as Li_2O or passive film (side-reaction byproducts of water and lithium). An ideal metallic nanoparticle formation is one in which the network is interconnected in the first charge/discharge cycle, because the network facilitates both charge-transfer reaction and electron conduction. In the 100 °C annealing electrode, the high hydrated water content may increase the thickness of the passive film around the metallic manganese particles, which in turn creates a high cell resistance, and consequently poor cycle-life performance. From Figure 9 it can be seen that as the annealing temperature of the electrodes increases, the corresponding cycle-life performance is enhanced. Yet after a threshold temperature of 300 °C, the electrodes differ very little in cycle-life performance, because the hydrated water content has pretty much been removed by 300 °C.

Conclusion

The synthesized manganese oxide electrodes are composed of interconnected nanowires. The diameter of nanowires after annealing at 100 and 300 °C is about 12−18 and 8−12 nm, respectively. The SAD pattern of the nanowires is a ring pattern indicating that these manganese oxide nanowires have poor crystalline structure. XRD and TEM results show that the higher the annealing temperature, the higher the crystallinity of the manganese oxide electrode. From TGA results, change in morphology and crystalline characteristics after heat treatment is attributed to the removal of both the surface and structural water from the solid phase of the manganese oxide structure. The reversible capacities in the first cycle of the 100, 300, and 500 °C annealing electrodes are about 600, 800, and 970 mAh g^{-1}, respectively. All electrodes demonstrate large irreversible capacity caused by the structural or textural modifications, the decomposition reactions of electrolyte, and the formation of the SEI film. The reaction mechanism of manganese oxide with lithium has been proposed as the formation/decomposition of Li_2O facilitated by metallic manganese. XPS results confirm the formation of Li_2O and metallic manganese after charging. In CV tests, the anodic peak is observed at about 1.2 V vs Li/Li^+ on the anodic process, and a sharp cathodic peak locates at 0.4 V vs Li/Li^+ on the cathodic process. The specific capacity of manganese oxide after 300 and 500 °C annealing decreases fast in the first 10 cycles, then decays to a nearly constant capacity onward. On the other hand, the capacity of the 100 °C annealing electrode decreases rapidly in the first 40 cycles, and decays to a very low capacity.

References and Notes

(1) Idota, Y.; Kubota, T.; Matsufuji, A.; Maekawa, Y.; Miyasaka, T. *Science* **1997**, *276*, 1395.

(2) Courtney, I. A.; Dahn, J. R. *J. Electrochem. Soc.* **1997**, *144*, 2045.

(3) Morales, J.; Sanchez, L. *J. Electrochem. Soc.* **1999**, *146*, 1640.

(4) Aurbach, D.; Nimberger, A.; Markovsky, B.; Levi, E.; Sominski, E.; Gedanken, A. *Chem. Mater.* **2002**, *14*, 4155.

(5) Ahn, H. J.; Choi, H. C.; Park, K. W.; Kim, S. B.; Sung, Y. E. *J. Phys. Chem. B* **2004**, 108, 9815.

(6) Poizot, P.; Laruelle, S.; Grugeon, S.; Dupont, L.; Tarascon, J.-M. *Nature* **2000**, *407*, 496.

(7) Poizot, P.; Laruelle, S.; Grugeon, S.; Dupont, L.; Tarascon, J.-M. *J. Power Sources* **2001**, *97*−*98*, 235.

(8) Wang, G. X.; Chen, Y.; Konstantinov, K.; Yao, J.; Ahn, J.; Liu, H. K.; Dou, S. X. *J. Alloys Compd.* **2002**, *340*, L5.

(9) Wang, Y.; Qin, Q. Z. *J. Electrochem. Soc.* **2002**, *149*, A873.

(10) Wu, M. S.; Chiang, P. C. *Electrochem. Solid-State Lett.* **2004**, *7*, A123.

(11) Wu, M. S.; Lee, J. T.; Wang, Y. Y.; Wan, C. C. *J. Phys. Chem. B* **2004**, *108*, 16331.

(12) Tench, D.; Warren, L. F. *J. Electrochem. Soc.* **1983**, *130*, 869.

(13) Pang, S. C.; Anderson, M. A.; Chapman, T. W. *J. Electrochem. Soc.* **2000**, *147*, 444.

(14) Omomo, Y.; Sasaki, T.; Watanabe, M. *Solid State Ionics* **2002**, *151*, 243.

(15) Preisler, E. *J. Appl. Electrochem.* **1976**, *6*, 311.

(16) Era, A.; Takehara, Z.; Yoshizawa, S. *Electrochim. Acta* **1967**, *12*, 1199.

(17) Preisler, E. *J. Appl. Electrochem.* **1976**, *6*, 301.

(18) Wu, M. S. *Appl. Phys. Lett.* **2005**, *87*, 153102.

(19) Dedryvere, R.; Laruelle, S.; Grugeon, S.; Poizot, P.; Gonbeau, D.; Tarascon, J.-M. *Chem. Mater.* **2004**, *16*, 1056.

(20) Wang, Y.; Zhang, Y. F.; Liu, H. R.; Yu, S. J.; Qin, Q. Z. *Electrochim. Acta* **2003**, *48*, A4253.